Annals of Hepatology 29 (2024) 101530

Contents lists available at ScienceDirect

Annals of Hepatology

journal homepage: www.elsevier.es/annalsofhepatology

Original article

Development of a biodegradable prosthesis through tissue engineering, for the organ-replacement or substitution of the extrahepatic bile duct

Alan I. Valderrama-Treviño[a], Andrés E. Castell-Rodríguez[b], Rolando Hernández-Muñoz[c], Nadia A. Vázquez-Torres[b], Andrés Macari-Jorge[d], Baltazar Barrera-Mera[e], Alfredo Maciel-Cerda[f], Ricardo Vera-Graziano[f], Natalia Nuño-Lámbarri[g,h,*], Eduardo E. Montalvo-Javé[h,i,j,*]

[a] Department of Angiology, Vascular and Endovascular Surgery. Hospital General de México. Dr. Eduardo Liceaga. Mexico City, Mexico
[b] Laboratory of experimental immunotherapy and tissue engineering. Faculty of Medicine. UNAM. CDMX. Mexico
[c] Department of Cell Biology and Development, Institute of Cellular Physiology, UNAM. CDMX. Mexico
[d] Department of Pathology, Medica Sur Hospital. CDMX, Mexico
[e] Department of Physiology. Faculty of Medicine. UNAM. CDMX. Mexico
[f] Materials Research Institute. UNAM. CDMX. Mexico
[g] Traslational Research Unit, Medica Sur Clinic & Foundation. Mexico City, Mexico
[h] Department of Surgery, Faculty of Medicine, The National Autonomous University of Mexico (UNAM). Mexico City, Mexico
[i] Hepato Pancreato and Biliary Clinic, Department of General Surgery, "Hospital General de Mexico", Dr. Eduardo Liceaga. Mexico City, Mexico
[j] Obesity and Digestive Diseases Unit, Medica Sur Clinic & Foundation. Mexico City, Mexico

ARTICLE INFO

Article History:
Received 14 March 2024
Accepted 3 July 2024
Available online 20 July 2024

Keywords:
Electrospinning
Bile duct disruption
Tissue engineering
Scaffold
Biodegradable nanofibers

ABSTRACT

Introduction and Objectives: There are different situations in which an extrahepatic bile duct replacement or substitute is needed, such as initial and localized stages of bile duct cancer, agenesis, stenosis, or bile duct disruption.
Materials and Methods: A prosthesis obtained by electrospinning composed of Poly (D,L-lactide-co-glycolide) (PGLA) - Polycaprolactone (PCL) - Gelatin (Gel) was developed, mechanical and biological tests were carried out to evaluate resistance to tension, biocompatibility, biodegradability, cytotoxicity, morphological analysis and cell culture. The obtained prosthesis was placed in the extrahepatic bile duct of 15 pigs with a 2-year follow-up. Liver function tests and cholangioscopy were evaluated during follow-up.
Results: Mechanical and biological evaluations indicate that this scaffold is biocompatible and biodegradable. The prosthesis implanted in the experimental model allowed cell adhesion, migration, and proliferation, maintaining bile duct permeability without altering liver function tests. Immunohistochemical analysis indicates the presence of biliary epithelium.
Conclusions: A tubular scaffold composed of electrospun PGLA-PCL-Gel nanofibers was used for the first time to replace the extrahepatic bile duct in pigs. Mechanical and biological evaluations indicate that this scaffold is biocompatible and biodegradable, making it an excellent candidate for use in bile ducts and potentially in other tissue engineering applications.

1. Introduction

In laparoscopic cholecystectomy, various structures can be inadvertently injured due to factors such as incorrect anatomical identification, incipient inflammatory processes, fibrosis, anatomical variations, and bleeding. Bile duct injuries during laparoscopic surgery are estimated to occur in 0.08–0.3 % of cases [1,2], and despite the expertise of surgeons, unforeseen complications may arise [3].

In the United States alone, approximately 750,000 cholecystectomies are performed annually, with around 2500 patients experiencing bile duct injuries. The tension-free Roux-en-Y hepatojejunostomy has emerged as a prominent treatment for such injuries, often considered the gold standard [3-6]. Nevertheless, there's ongoing exploration of alternative therapeutic approaches. Experimental treatments, including the utilization of scaffolds to provide structural support for cell adhesion and growth, have been investigated. These

Abbreviations: PGLA, Poly D, L-lactide-co-glycolide; PCL, Polycaprolactone; Gel, gelatin; TFE, 2,2,2-trifluoroethanol; HFIP, 1,1,1,3,3,3-Hexafluoro-2-propanol; FTIR, Fourier transform infrared spectroscopy

* Corresponding authors.
E-mail addresses: nlambarri@gmail.com (N. Nuño-Lámbarri), montalvoeduardo@hotmail.com (E.E. Montalvo-Javé).

https://doi.org/10.1016/j.aohep.2024.101530

scaffolds aim to promote the development of subsequent tissue, aiding in the repair of damaged bile ducts [7].

Tissue engineering plays a pivotal role in this realm, involving the combination of scaffolds, cells, and biologically active molecules to create functional tissues. Various materials, both natural and synthetic polymers, are employed in scaffold fabrication to mimic the extracellular matrix, facilitating cell adhesion and migration, and ultimately promoting tissue regeneration [8-12]. Electrospinning, a technique capable of producing nanofibers from different materials and incorporating growth factors or bioactive molecules, has emerged as a promising approach in tissue engineering [7,13]. Nanofibers offer unique characteristics such as a high surface area-to-volume ratio, porosity, and mechanical properties, rendering them attractive for biomedical applications [14].

This study reports the pioneering development and application of an electrospun tubular scaffold comprising Poly (D,L-lactide-co-glycolide) (PGLA), Polycaprolactone (PCL), and Gelatin (Gel) for extrahepatic bile duct replacement. Such innovative approaches hold the potential to significantly advance the field of bile duct injury treatment and repair.

2. Materials and Methods

2.1. Biodegradable prosthesis

Using the electrospinning technique, the following biopolymers were used: PCL Mw= 80,000 (Sigma Aldrich), PGLA Mw= 66,000–107,000 (Sigma Aldrich), GEL TYPE B bovine skin (Sigma Aldrich). The solvents used for PCL and PGLA were 2,2,2-trifluoroethanol (TFE), and the solvent for GEL was 1,1,1,3,3,3-Hexafluoro-2-propanol (HFIP). For the preparation of the viscoelastic polymer solution, PGLA-PCL 70:30 with the solvent TFE (19% w/v) was used and mixed for 24 h, for PGLA-PCL/Gel ratio was 80:20, with the HFIP solvent (10% w/v), and they were mixed for 12 h with a magnetic stirrer. The polymer solution was added to a 5 ml plastic syringe with a 21 G non-cutting needle with dynamic collector.

2.2. Fourier transform infrared spectroscopy (FTIR) and Young's modulus

To determine the presence of the PGLA-PCL-Gel functional groups present in the scaffold obtained by electrospinning, FTIR spectroscopy was used with a Thermo Nicolet NEXUS 670 FTIR spectrophotometer from the Materials Research Institute of the UNAM. The spectrum obtained ranged between 500 and 4000cm^{-1}.

Indentation and relaxation measurements were performed on cylindrical electrospun PGLA-PCL-Gel samples mounted on a slide with double-sided tape and moistened with saline solution for measurement. Indentation and relaxation measurements were carried out on each sample. The data were analyzed using the Hertz model for indentation and the generalized Maxwell model for relaxation. The indentation data were fitted to the Hertz model with a maximum indentation distance of 7.5 μm to calculate Young's modulus with the Femto Tools FT-MTA03 equipment with an FT-S200 tip with a 50 μm diameter glass sphere at the tip.

2.3. Scanning electron microscopy

The morphological characteristics of the scaffold generated by electrospinning were obtained with the Schottky-type field emission scanning electron microscopy technique and with JEOL model JSM-7600F scanning electron microscopy. Fiber diameter and pore size were determined with Image J software.

2.4. Contact angle

To evaluate the hydrophilic properties of the scaffold, the contact angle measurement was carried out with a Ramé-Hart Instrument Co. model 100–07 goniometer. 5μl of distilled water was placed, and the contact angles were measured with the ImageJ program at 1.60 and 300 s.

2.5. In vitro *degradation and cell culture*

The degradability tests were conducted in PBS solution with pH 7.4 and human bile with pH 7.0 at 37 °C; weight measurements were taken at 2, 3, and 4 months. They were dried and weighed accurately, and the initial weight was compared with the final weight. The degradation rate was calculated with the following formula: [15,16]

$$\text{weight loss } (\%) = \frac{M0 - Mt}{M0} \times 100$$

M0 and Mt are the sample weights before and after incubation in PBS/bile solution.

Before cell culture, the scaffolds were immersed for 24 h in 70 % alcohol for sterilization. Fibroblasts were seeded on the cell surface of the PGLA-PCL-Gel scaffold with a cell density of 10×10^4 per cm^2. Dulbecco's Modified Eagle's/Ham's Nutrient Mixture F12 BIOWEST culture medium, BIOWEST fetal bovine serum was used, the culture medium was replaced every three days, and the samples were kept in a tissue culture incubator at 37 °C with 5 % CO2. Cell viability was determined by the fluorescence of calcein and cell death with the ethidium homodimer that indicated cell permeability (THERMO FISHER SCIENTIFIC live/dead Kit).

2.6. In vivo *biocompatibility*

3 New Zealand breed rabbits weighing 2.5–3.5 kg were used to evaluate biocompatibility. They were housed and managed according to the Mexican Official Standard-062-Z00 [17]. Samples of the PGLA-PCL-Gel scaffold were implanted in the subcutaneous cellular tissue of the back of the rabbits, with follow-up at 60 days.

2.7. Anesthesia and surgical procedure

15 Female Landrace pigs weighing 25 kg were used. Follow-up was carried out with blood samples at months 1,3,6,12, and 18 months. The ARRIVE 2.0 guidelines were incorporated into the management and care of the animals [18].

The sedation was induced using Sural from Lab. Chinoin®, dosed at 2 mg/kg administered intramuscularly (IM).

Cannulation of the marginal ear vein was conducted using a 20Fr catheter for intravenous (IV) administration of pentobarbital from Lab. Pets Pharma, dosed at 40 mg/kg. An endotracheal tube was inserted to secure the airway, assisted by a Harvard automatic ventilator. Continuous monitoring included heart rate, blood pressure, oxygen saturation (SpO_2), and capnography.

Before extubation, 100 % FiO_2 was administered, and oropharyngeal secretions were aspirated under direct vision. Neuromuscular relaxants were antagonized, positive pressure was applied, the pneumatic tamponade was deflated, and extubation was performed. Animals were then transferred to the postoperative recovery unit for continued monitoring.

One hour before surgery, prophylactic administration of enrofloxacin from Pisa (1 g IM) was carried out. During immobilization in the supine position, a mid-supraumbilical incision was made. The gallbladder and extrahepatic bile duct were identified, followed by a cross-section of the common bile duct. An end-to-end common bile duct-prosthesis-bile duct anastomosis was performed using PDS 5–0 Ethicon sutures in simple interrupted stitches. Postoperatively,

analgesic Meloxicam (Biochem 500 mg/12 hrs/3 days IM) and antibiotic enrofloxacin (1 g/24 hrs/7 days) were administered.

2.8. Liver function tests

Blood samples were taken 24 h before the surgical procedure and 1, 3, 6, 12, and 18 months after the procedure to quantify liver function tests such as aspartate aminotransferase, alkaline phosphatase, and total bilirubin. Each sample was obtained in an Eppendorf tube and was processed with the Universal Kit, Bayer Leverkusen.

2.9. Histopathological study and immunohistochemistry

Bile duct biopsies were obtained in accordance with the guidelines set forth by the National Institutes of Health, the Institutional Review Board of the Roswell Park Cancer Institute, and the University of North Carolina School of Medicine at Chapel Hill. These biopsies encompassed the region where the prosthesis was implanted and were preserved in buffered formalin. Following fixation, the tissue sections were embedded in paraffin and subjected to a heat treatment at 70 °C for 20 min. Deparaffinization was achieved using xylene, followed by rehydration through graded alcohols in a phosphate buffer solution.

Evaluation of common bile duct regeneration involved the assessment of biliary epithelium, intramural glands, and the presence of inflammatory and fibrous tissue at the prosthesis insertion site. Hematoxylin-Eosin staining was employed for this purpose.

Endogenous peroxidase activity was quenched by incubating the slides in 3 % H_2O_2 for 6 min at room temperature. Antigen retrieval was performed by immersing the slides in 0.01 sodium citrate (pH 6.0) for 20 min in a microwave oven at high temperature, followed by a 15-minute cooling period in the citrate solution. Subsequently, the slides were incubated with primary antibodies, including BioSB MUC5AC (1:100) from Biocare and CK 19 (1:100) from BioSB, for 1 hour at room temperature. After incubation, the slides were washed thrice with Tris-buffered Saline.

Detection of the primary antibodies was accomplished using the BioSB kit with BIOTIN/STREPTAVIDIN, followed by incubation with 3,3′ Diaminobenzidine for 8 min at room temperature. Counterstaining was performed with hematoxylin and Hycel. Images were captured and stored using APERIO and ImageScope software.

2.10. SpyGlass™

For the SpyGlass study, the animals were anesthetized with the previously described anesthetic protocol; an endoscopic guide was used to canalize Vater's ampulla. The SpySscope™ DS was used, with direct visualization equipment, Boston Scientific Corp. We advanced towards the bile duct of the pigs, observing the common bile duct and extrahepatic bile duct.

2.11. Statistical analysis

For the statistical analysis of the liver function tests, the IBM SPSS Statistics version 29.0.2.0 program was used. Means and standard deviations were calculated, ANOVA tests were performed, and a p-value of less than 0.05 was considered statistically significant.

2.12. Ethical considerations

The protocol was approved by the Ethics and Research Committees of the National Autonomous University of Mexico and the General Hospital of Mexico "Dr. "Eduardo Liceaga." The animals were cared for in independent cages, managed, and anesthetized according to the Official Mexican Standard 062-ZOO-1999 [17].

3. Results

3.1. Biodegradable prostheses

The electrospinning variables were adjusted with an output flow of 1.2 ml/hr at 10 cm between the needle tip and the dynamic collector. The needle-positive pole was connected to 14 kV, and the negative pole to the dynamic collector was maintained at a constant speed of 3800 rpm. Optical microscopy evaluated the absence of bulbs and continuous fibers for the initial analysis of the fiber morphology. (Fig. 1) The dynamic collector had a diameter of 0.3 cm and a length of 12 cm. A scaffold with a length of 9 cm and an internal diameter of 0.3 cm was obtained. The ends were removed and cut into sections of 2−3 cm to carry out mechanical and biological tests.

3.2. FTIR

FTIR spectroscopy was performed to study the chemical structure of synthetic polymers. The spectral result obtained from the PGLA-PCL-Gel polymers is shown separately and combined in Fig. 2.

The characteristic spectra of pure PCL were found in the bands 1723cm^{-1}, corresponding to the C = O carbonyl bond in stretching mode. The band 2867cm^{-1} corresponds to a symmetric stretching of methylene (CH_2), and at 2941 cm^{-1}, the asymmetric stretching band of CH_2 is found, which coincides with Sánchez *et al.* [19] In the PGLA-PCL-Gel scaffold the PCL spectrum remained at 1723cm^{-1} with slight variation at 2852cm^{-1} and 2944cm^{-1}. Amide I, II, and III are characteristic of the molecular structure of gelatin; the slight difference in the spectra in the intensity and frequency of the samples may be due to the conformational differences of the polypeptide chain [20].

Peaks for Amida I were obtained in the regions 1628cm^{-1} when the polymer was pure and at 1637cm^{-1} with the final structure of the PGLA-PCL-Gel scaffold, coinciding with previous reports where it is demonstrated that the spectrum of Amida I of gelatin is absorbed between 1700 and 1600cm^{-1} [21]. Amide I represent a combination of C = O stretching vibrations that are hydrogen bonding with COO, CN stretching, CCN deformation and NH bending. For the spectrum of Amida II, peaks were obtained at 1530cm^{-1} when the polymer was pure and 1540cm^{-1} in the final structure of the scaffold; the spectrum of Amida II is absorbed between 1500 and 1560cm^{-1} [22] and corresponds to the vibrational changes of -CN stretching and -NH bending of the peptide group. For the spectrum of amide III, peaks were obtained at 1234cm^{-1} with the pure polymer and 1239cm^{-1} in the final structure of the scaffold; the spectrum of Amida III is absorbed between 1269 and 1080cm^{-1} [20]. In general, the spectrum of Amide III indicates a disorder in the molecular structure of gelatin, associated with the loss of the triple helical state [23]. PLGA has characteristic bands at 1100−1250cm^{-1} and 1750−1760cm^{-1}, representing the ester and carbonyl groups respectively [16]. The spectrum obtained with pure PLGA was 1179−1743cm^{-1}, in the final scaffold structure, the spectrum obtained was 1179, 1750 cm^{-1}.

3.3. Young's modulus

As shown in Fig. 2E, the material relaxes quickly since, after 50 s, it has practically reached its maximum relaxation. This is seen in the relaxation time spectrum where there are two contributions at very long times, small ones and one more at 11 s. (Fig. 2F) The average Young's modulus was 852.1 kPa, with a standard deviation of 114.50 kPa. The behavior of the dynamic modules shows the losses (red color) and storage (green color). (Fig. 2G)

3.4. Scanning electron microscopy

Fig. 3 shows images obtained by SEM of the electrospun scaffold composed of PGLA-PCL-Gel; the presence of bulbs or discontinuous

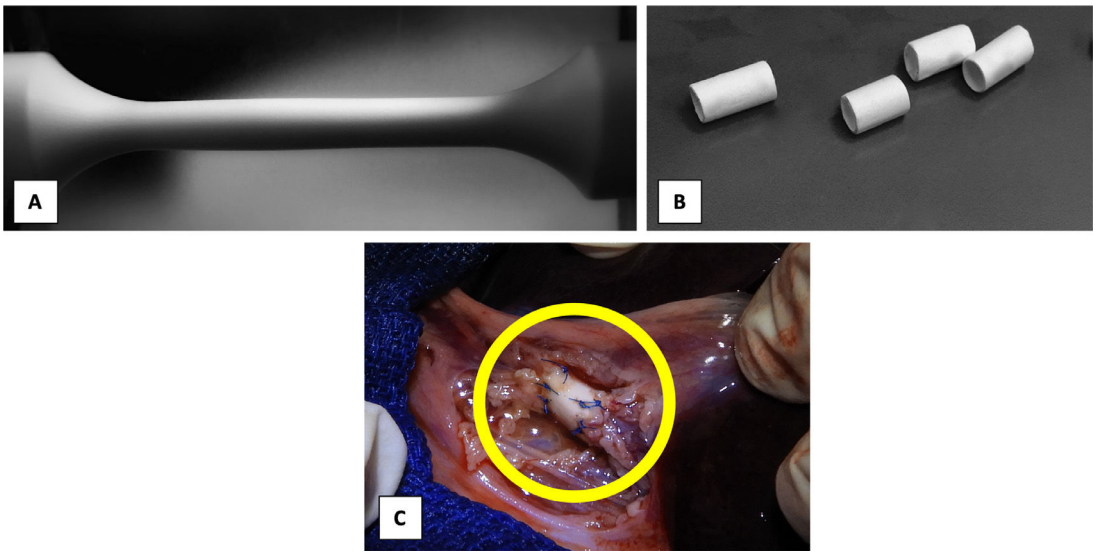

Fig. 1. Scaffold obtained by electrospinning. A), fibers collected in dynamic collector. B), 2–3 cm sections for mechanical-biological evaluations. C) End-to-end anastomosis: common bile duct-prosthesis-common bile duct.

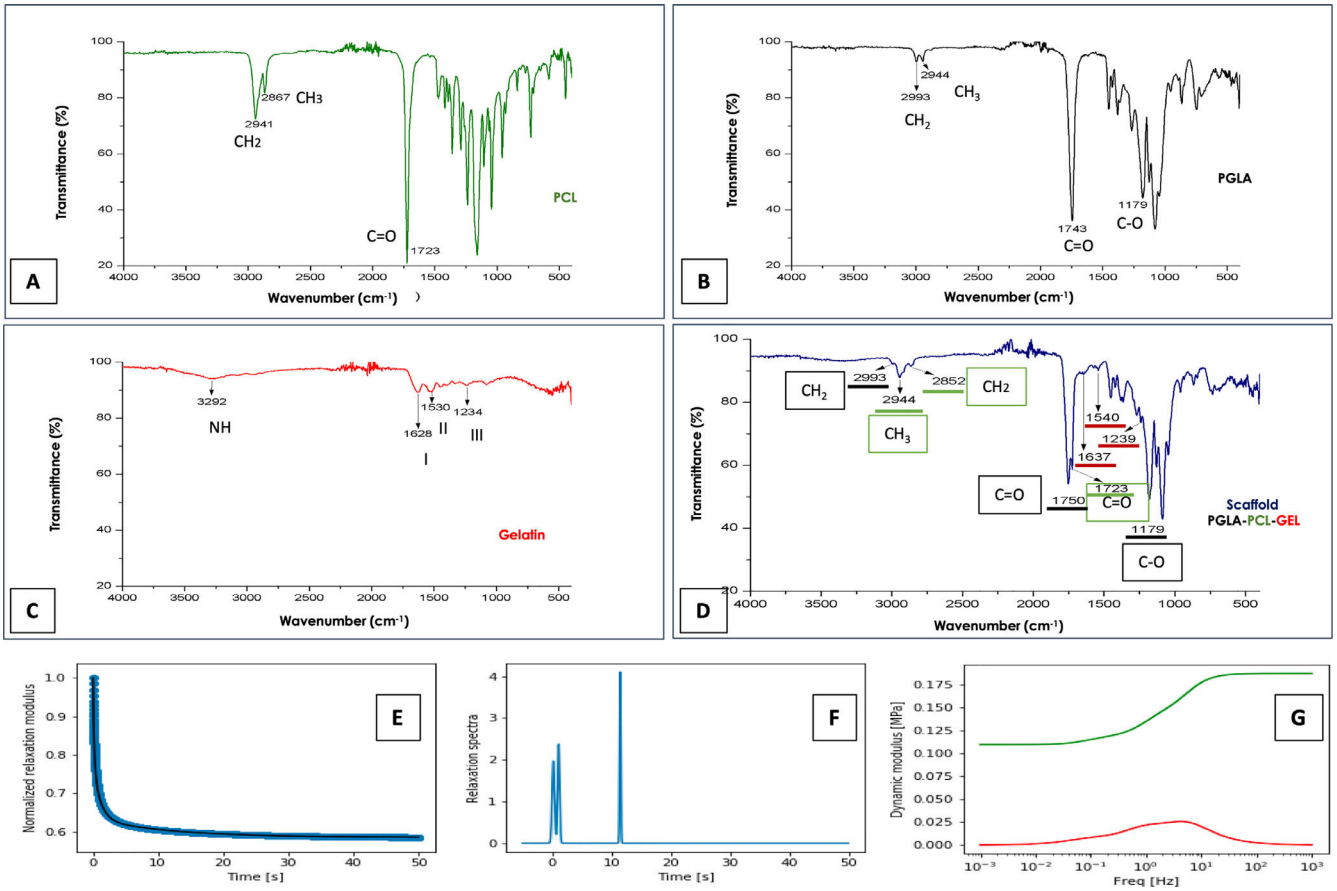

Fig. 2. FTIR spectroscopy and mechanical tests. Spectrum of the polymers PCL, Figure A. Figure B, PLGA. Figure C, Gelatin. In Figure D, the spectrum of the electrospun scaffold, characteristic functional groups of the 3 polymers is observed. Figure E, Relaxation test. Figure F, Spectrum of relaxation times. Figure G, dynamic modules behavior; red color losses, green color storage.

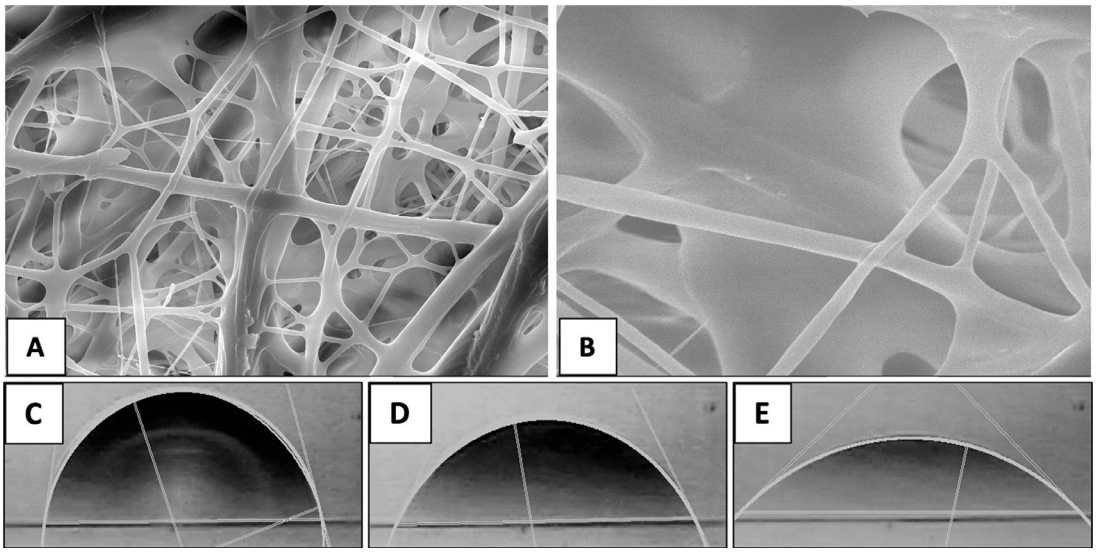

Fig. 3. SEM of the scaffold and contact angle. Figures A and B. Morphological analysis by SEM. Figures C, D, and E. Measurement of the contact angle at seconds 1, 60 and 300 respectively.

fibers is not observed. The average diameter of the electrospun fibers was 51 μm with a standard deviation of 0.19 μm, and the average pore (interfibrillar distance) was 2.72 μm with a standard deviation of 1.9 μm.

3.5. Contact angle

To determine the contact angle, a drop of distilled water was deposited on the scaffold composed of PGLA-PCL-Gel and images were taken for 6 min, of which 3 times were chosen: 1-, 60- and 300-seconds. (Fig. 3) The determination of the theoretical contact angle of the PGLA-PCL-Adamium Gel was 77.7° at second 1, 61.1° at second 60 and 42° at 300 s, after 300 s the drop spread on the polymeric scaffold (hydrophilic surface).

3.6. In vitro *degradation*

The weight loss percentage in the scaffolds immersed in bile at two months was 16.2 %, at three months 57.1 %, and 74.4 % at four months. The weight loss percentage in the scaffolds immersed in physiological solution at two months was 60.6 %; at three months, it was 68 %, and at four months, it was 81 %.

3.7. Cell culture

The evaluation of the PGLA-PCL-Gel scaffold cytotoxicity was carried out with the calcein/etideum homodimer kit. Cell counting was done at 600μm^2 of different samples with the ImageJ program, and the average percentage of cell viability was determined at 2, 8 and 10 days. Fig. 4 shows fibroblast growth on the scaffold after ten days. The average percentage of cell viability at 2.8 and 10 days was 98.5 %, 95.4 %, and 93.5 %, respectively, with a mortality rate at 2.8 and 10 days of 1.5 %, 4.6 %, and 6.5 %. The combined images of cell viability and death are observed.

3.8. In vivo *biocompatibility*

Sections of the scaffold were implanted into the subcutaneous cellular tissue on the rabbits' backs, and control of gauze sections. Samples were obtained at 7, 23, and 44 days. (Fig. 5) A panoramic view of soft tissues is observed with chronic granulomatous inflammation as a foreign body type (gauze textile fibers), with fibrosis. Multinucleated giant cells are seen phagocytosing foreign material. On day 7, epithelialization of the scaffold was identified with minor inflammation; on day 23, complete lining epithelium was observed without inflammation or interstitial fibrosis; on day 44, no inflammation or dermal reaction to the scaffold was identified and epithelialization continued.

3.8.1. Surgical procedure

With general anesthesia, animals were immobilized with limb restraints in the supine position. A mid-supraumbilical incision was made, dissection was performed in planes, verifying hemostasis until reaching the gallbladder, which we used as a reference to identify the common bile duct. The gallbladder and the extrahepatic bile duct were identified, a cross-section was made in the common bile duct, and an end-to-end common bile duct-prosthesis-bile duct anastomosis was performed with PDS 5−0 Ethicon suture, using simple separated stitches. (Fig. 1C) Absence of bile fluid leak was verified, and a Penrose-type drain was placed and removed after 24 hrs. Analgesic Meloxicam Biochem 500 mg/12 hrs/3 days IM and antibiotic enrofloxacin 1 g/24 hrs/7 days were administered.

3.9. Liver function tests

The mean values of liver function tests, including alkaline phosphatase, total bilirubin, and aspartate aminotransferase, showed no statistically significant differences throughout the entire study. (Table 1)

3.10. SpyGlass^{TM}

For the internal visualization of the bile duct, SpyGlassTM was performed, and no trace of the prosthesis was observed after eight months. The extrahepatic bile duct was found to be patent without signs of obstruction or stenosis, with follow-up at 18 months. (Fig. 6)

3.11. Immunohistochemistry MUC5AC, cytokeratin 19

Follow-up was given for 18 months, and a biopsy of the extrahepatic bile duct was performed, where the presence of biliary epithelium, intramural glands, and smooth muscle fibers was observed.

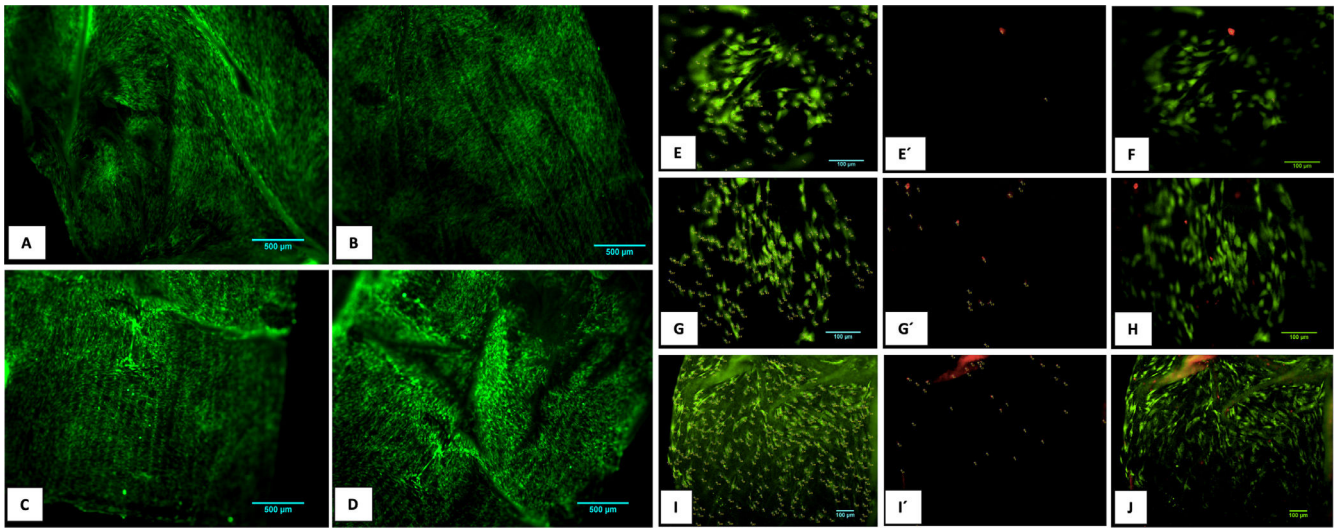

Fig. 4. Cell viability. Fibroblast growth after 10 days. Figures A, B, C, D, E, G, and I alive/dead test positive for calcein. Figures E, G, I, positive for ethidium homodimer. Figures F, H, and J MERGE.

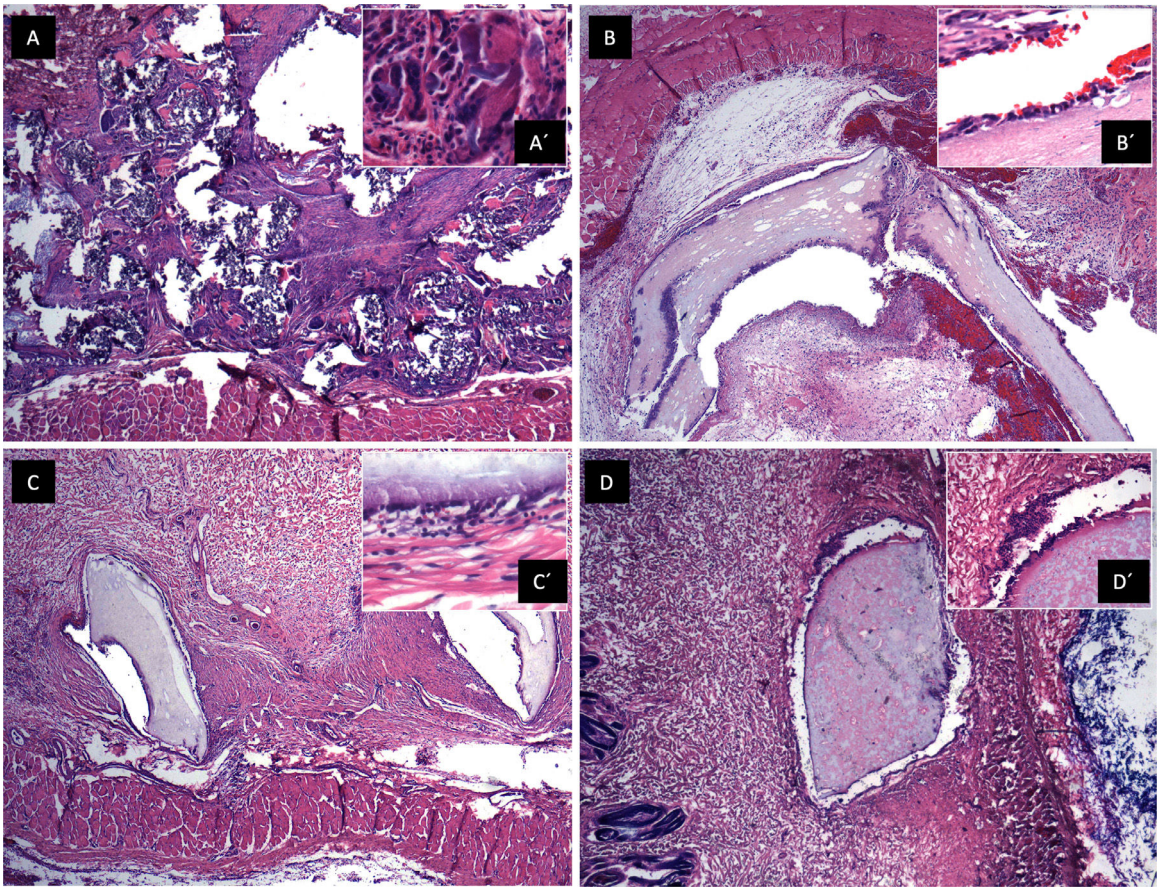

Fig. 5. Biocompatibility *in vivo*. A. Panoramic view of a soft tissue section 44 days after gauze placement in subcutaneous cellular tissue, H&E technique. Chronic granulomatous inflammation of the foreign body type (textile fibers) with fibrosis is observed. A' (100x magnification), multinucleated giant cells are observed phagocytosing foreign material. B. Skeletal muscle soft tissue panoramic view,7 days after placing the scaffold in subcutaneous cellular tissue, H&E technique. Scaffold epithelialization with hemorrhage is observed. B' (100x magnification), epithelium is observed on the scaffold, with little inflammation. C. Panoramic view after 23 days where lining epithelium is observed on the scaffold, no inflammation or interstitial fibrosis is observed in the dermis. C' (100x magnification), a scaffold covered with epithelium is observed with minimal non-specific chronic inflammation and hemorrhage. D. Panoramic view after 44 days, no inflammation or dermal reaction to the scaffold is identified. D' (100x magnification), epithelialization of the scaffold, no inflammation is identified.

Table 1
Liver function test means throughout the study.

	Initial sample ± SD	First month ± SD	Third month ± SD	Sixth month ± SD	Twelfth month ± SD	Eighteenth month ± SD	p-value
Alkaline Phosphatase	171.80 ± 4.44	171.46 ± 4.24	170.83 ± 4.08	170.33 ± 3.87	171.80 ± 4.44	171.00 ± 7	0.945
Total Bilirubin	0.092 ± 0.023	0.090 ± 0.026	0.098 ± 0.018	0.084 ± 0.025	0.090 ± 0.029	0.090 ± 0.020	0.873
Aspartate Aminotransferase	19.46 ± 1.45	19.68 ± 1.32	19.74 ± 1.70	19.24 ± 1.49	18.96 ± 1.67	18.20 ± 0.95	0.548

Abbreviations: **SD**, Standard deviation.

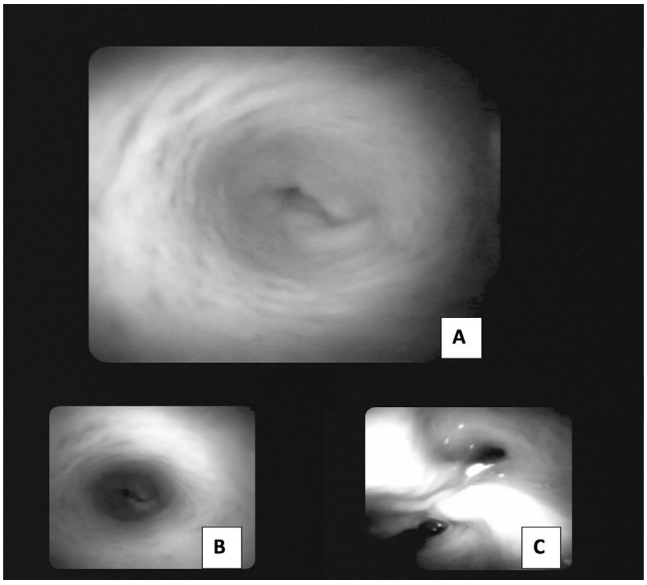

Fig. 6. SpyGlass. Figures A and B. Internal visualization of the bile duct with follow-up at 18 months, the re-epithelialized scaffold wall is observed in the common bile duct area. Figure C. Bifurcation of the left and right hepatic ducts.

Cytoplasmic positivity was found in epithelial cells for MUC5AC, and membrane positivity with CK19 in luminal and intraluminal epithelial cells. (Fig. 7)

4. Discussion

In this study, clinical and laboratory follow-up is given to porcine models that underwent surgery to replace the common bile duct with a biodegradable prosthesis composed of the synthetic polymers PGLA-PCL-Gel, which was created by electrospinning that fulfills a scaffold function. Generally, cellular affinity towards synthetic polymers is low due to their high hydrophobicity and the few or no cellular recognition sites, which is why strategies have been innovated to improve hydrophilic properties, such as the incorporation of hydrophilic polymers, bioactive molecules, growth factors or sites of cell recognition [24,25] such as the arginine-glycine-aspartic acid sequences that gelatin characteristically possesses, which facilitates cell migration and adhesion, is also biodegradable, biocompatible and does not present immunogenicity compared to collagen.

Polycaprolactone is a material commonly used in the creation of scaffolds; [26] however, it has a contact angle of 132°, which results in a hydrophobic surface [27,28] that, when treated with gas plasma or gelatin, the hydrophilicity of the PCL scaffolds is improved [29]. In our study, the decrease in the PCL contact angle is considerably noted when combined with hydrophilic polymers, which generally improves the properties of the scaffolds, such as resistance, high porosity, and bioactivity, favoring cell adhesion and its degradation within the organism [19,30,31]. The amide groups' appearance in the FTIR spectra of the electrospun PGLA-PCL-Gel scaffolds indicates that the PCL-PGLA chains were chemically attached to the gelatin molecules and led to the introduction of functional groups such as NH_2 and COOH [24,25,28]. The scaffolds obtained through the electrospinning process can mimic the extracellular matrix because it allows the production of nanometric or micrometric fibers, in which a wide variety of polymers can be used [32], including those used in this study, in addition to being approved by the FDA [33,34].

Different studies have reported the importance of artificial scaffolds in tissue engineering, which could be used to treat multiple diseases [11,29,35-37], where the application of nanofibers has increased due to their more significant interaction between scaffold cells [38,39]. This study demonstrated the effectiveness of a PGLA-PCL-Gel scaffold created by electrospinning to replace the

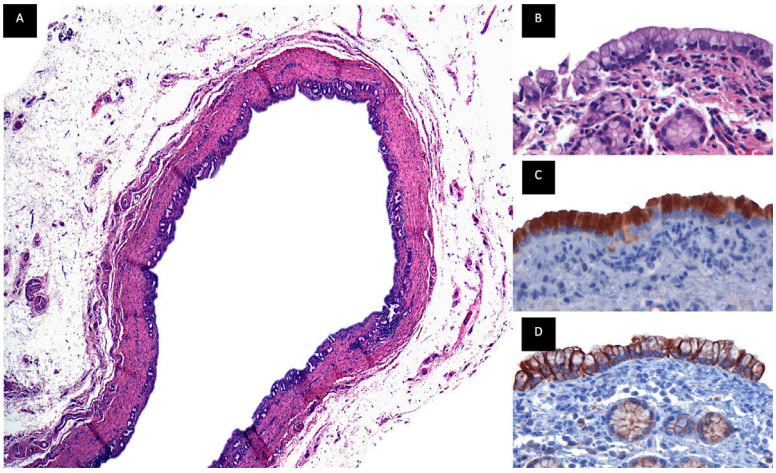

Fig. 7. Immunohistochemistry. Common bile duct biopsy that was replaced by the PGLA-PCL-Gel scaffold with 18-month follow-up. Figure A. Panoramic view of duct lined by a biliary-type epithelium with intramural glands, the wall of the duct is composed of smooth muscle fibers, beneath the muscular wall a layer of adipose tissue rich in blood vessels and nerves is identified, H&E technique. Figure B. (100x), epithelium of biliary morphology with round to oval nuclei of basal location with preserved polarity, below the epithelium the muscle wall with intramural glands of biliary phenotype is observed. Figure C. (100x), immunoreaction for MUC5AC, cytoplasmic positivity is observed in the epithelial cells. Figure D (100x), immunoreaction for CK19, membrane positivity is observed in the luminal and intramural epithelial cells.

extrahepatic bile duct with satisfactory mechanical and biological tests for its use and application *in vivo*. In the experimental model, the sectioned area was covered by biliary epithelium, and according to histopathological analysis, there were no giant cells, fibrosis, or inflammation. Clinical follow-up and blood samples demonstrated adequate bile flow without stenosis or obstruction, corroborated by SpyGlass and the analysis of liver enzymes, which remained within a normal range.

The process of elaboration and design of a biodegradable scaffold requires careful planning, starting with the choice of polymers, the characterization of the electrospinning process, the mechanical and biological analysis, the possible cytotoxicity in cell culture or the surgical technique could represent various complications. Additionally, the main complications after placement of the scaffold in the extrahepatic bile duct are directly related to bile flow, since in the event of obstruction of the biliary drainage system, cholangitis, bile leak, biloperitoneum, sepsis, shock and death could occur.

5. Conclusions

In this study, a tubular scaffold composed of electrospun PGLA-PCL-Gel nanofibers was used for the first time to replace of the extrahepatic bile duct in pigs. Mechanical and biological evaluations indicate that this scaffold is biocompatible and biodegradable, making it an excellent candidate for bile duct injuries and potentially other tissue engineering applications.

Funding

This research did not receive any specific grant from funding agencies in the public, commercial, or not-for-profit sectors.

Authors contributions

AIVT, study design, literature review, data collection, variable analysis, carried out the experiment, manuscript writing; AECR, conceived the original idea, study design, literature review, data collection, variable analysis, carried out the experiment, manuscript writing; RHM, study design, supervised the project, data collection, variable analysis; NAVT, carried out the experiments, adjustments and design in electrospinning process, cell culture, study design, literature review, data collection, variable analysis; AMJ, histopathological analysis, literature review, data collection, variable analysis; BBM, Analysis and interpretation of results, literature review, data collection, variable analysis; AMC, Analysis and interpretation of results, adjustments, and design in electrospinning process; RVG, Analysis and interpretation of results, adjustments, and design in electrospinning process; NNL, Literature review, data collection, variable analysis, manuscript writing; EEMJ, Conceived the original idea, study design, literature review, data collection, variable analysis, carried out the experiment, manuscript writing.

Conflicts of interest

None.

Acknowledgments

Alan Isaac Valderrama-Treviño is a doctoral student from the Programa de Doctorado en Ciencias Biomédicas at the Universidad Nacional Autónoma de México (UNAM) and received CONAHCYT 694871 scholarship.

References

[1] Halbert C, Pagkratis S, Yang J, Meng Z, Altieri MS, Parikh P, et al. Beyond the learning curve: incidence of bile duct injuries following laparoscopic cholecystectomy normalize to open in the modern era. Surg Endosc 2016;30:2239–43. https://doi.org/10.1007/s00464-015-4485-2.
[2] Mangieri CW, Hendren BP, Strode MA, Bandera BC, Faler BJ. Bile duct injuries (BDI) in the advanced laparoscopic cholecystectomy era. Surg Endosc 2019;33 (3):724–30 3. https://doi.org/10.1007/s00464-018-6333-7.
[3] Sicklick JK, Camp MS, Lillemoe KD, Melton GB, Yeo CJ, Campbell KA, et al. Surgical management of bile duct injuries sustained during laparoscopic cholecystectomy: perioperative results in 200 patients. Ann Surg 2005;241:786–92. https://doi.org/10.1097/01.sla.0000161029.27410.71.
[4] Kapoor VK. Management of bile duct injuries: a practical approach. Am Surg 2009;75:1157–60. https://doi.org/10.1177/000313480907501.
[5] Sahajpal AK, Chow SC, Dixon E, Greig PD, Gallinger S, Wei AC. Bile duct injuries associated with laparoscopic cholecystectomy: timing of repair and long-term outcomes. Arch Surg 2010;145:757–63. https://doi.org/10.1001/archsurg.2010.153.
[6] Sushruth S, Premal RD, Hasmukh BV, Mahendra SB, Lakshman SK, Ajay Y, et al. Management of Major Postcholecystectomy Biliary Injuries. J Surg 2019;25 (1):91–6. https://doi.org/10.4103/njs.NJS_35_18.
[7] Chan BP, Leong KW. Scaffolding in tissue engineering: general approaches and tissue-specific considerations. Eur Spine J 2008;17(4):467–79. https://doi.org/10.1007/s00586-008-0745-3.
[8] Michael R, Jeffrey P, Robert P, Alicia F, Fred B, Frank D. Small intestinal submucosa as a bioscaffold for biliary tract regeneration. Surgery 2002;132(3):480–6. https://doi.org/10.1067/msy.2002.126505.
[9] Fotios S, Alexander WJ, Olivia CT, Stephen S, Edmund MG, Sara SU, et al. Reconstruction of the mouse extrahepatic biliary tree using primary human extrahepatic cholangiocyte organoids. NatMed 2017;23(8):954–63. https://doi.org/10.1038/nm.4360.
[10] Griffith LG, Naughton G. Tissue engineeringcurrent challenges and expanding opportunities. Science 2002;295(5557):1009–14. https://doi.org/10.1126/science.1069210.
[11] Valderrama A, Uriarte K, Granados JJ, Rodriguez AE, Maciel A, Banegas R, et al. Tubular electrospun scaffolds tested in vivo for tissue engineering. Int J Res Med Sci 2019;7:635–43. https://doi.org/10.18203/2320-6012.ijrms20190373.
[12] Ma XP. Biomimmetic materials for tissue engineering. NIH 2008;60(2):184–98. https://doi.org/10.1016/j.addr.2007.08.041.
[13] Teo W, Ramakrishna S. A review on electrospinning design and nanofiber assemblies. Nanotechnol 2006;17(14):R89–R106. https://doi.org/10.1088/0957-4484/17/14/R01.
[14] Duque LM, Rodriguez L, López M. Electrospinning: la era de las nanofibras. Rev. lber. Polímeros. 2014;14(1):10–27.
[15] Powell H, Supp D, Boyce S. Influence of electrospun collagen on wound contraction of engineered skin substitutes. Biomaterials 2008;29:834–43. https://doi.org/10.1016/j.biomaterials.2007.10.036.
[16] Alireza S, Samira N, Amir M, Mohammad K, Meysam M. Synthesis and characterization of collagen/PLGA biodegradable skin scaffold fibers. Regen Biomater 2017:309–14. https://doi.org/10.1093/rb/rbx026.
[17] Norma Oficial Mexicana. Especificaciones Técnicas para la producción, cuidado y uso de los animales de laboratorio. NOM-062-ZOO- 1999.
[18] Percie du Sert N, Hurst V, Ahluwalia A, Alam S, Avey MT, Baker M, et al. The ARRIVE guidelines 2.0: updated guidelines for reporting animal research. PLoS Biol 2020;18(7):e3000410. https://doi.org/10.1371/journal.pbio.3000410.
[19] Sánchez A, Vera R, Muñoz E, Gómez E, Bernad M, Maciel A. Preparation and characterization of electrospun polymeric membranes of polycaprolactone and chitosan for controlled release of thiamine chlorhydrate. Ciencia en Desarrollo 2016;7:133–51.
[20] Meliana W, Nurul J, Perry B, Lukman A. Physical and chemical properties of gelatin from red snapper scales: temperature effects. JURNAL TEKNIK 2019;8:95–101. https://doi.org/10.12962/j23373539.v8i2.49703.
[21] Muyonga J, Cole C, Duodu K. Extraction and physico-chemical characterisation of Nile perch (Lates niloticus) skin and bone gelatin. Food Hydrocoll. 2004;18:581–92. https://doi.org/10.1111/j.1750-3841.2009.01106.x.
[22] Yakimets I, Wellner N, Smith A, Wilson R, Farhat I, Mitchell J. Mechanical properties with respect to water content of gelatin films in glassy state. Polymer (Guildf) 2005;46:12577–85. https://doi.org/10.1016/J.POLYMER.2005.10.090.
[23] Wulandari D, Monica R. Pembuatan masker wajah peel off berbasis gelatin dari sisik ikan kakap merah dengan metode hidrolisis. Institut Teknologi Sepuluh Nopember; 2017.
[24] Ma Z, He W, Yong T, Ramakrishna S. Grafting of gelatin on electrospun poly (caprolactone) nanofibers to improve endothelial cell spreading and proliferation and to control cell orientation. Tissue Eng. 2005;11(7–8):1149–58. https://doi.org/10.1089/ten.2005.11.1149.
[25] Zhu Y, Gao C, Shen J. Surface modification of polycaprolactone with poly (methacrylic acid) and gelatin covalent immobilization for promoting its cytocompatibility. Biomaterials 2002;23(24):4889–95. https://doi.org/10.1016/s0142-9612(02)00247-8.
[26] Fukunishi T, Best C, Sugiura T, Opfermann J, Ong CS, Shinoka T, et al. Preclinical study of patient-specific cell-free nanofiber tissue-engineered vascular grafts using 3-dimensional printing in a sheep model. J Thorac Cardiovasc Surg 2017;153(4):924–32. https://doi.org/10.1016/j.jtcvs.2016.10.066.

[27] Park H, Lee K, Lee S, Park K, Park W. Plasma-treated poly (lactic-co-glycolic acid) nanofibers for tissue engineering. Macromol Res 2007;15(3):238–43. https://doi.org/10.1007/BF03218782.
[28] Zander N, Orlicki J, Rawlett A, Beebe T. Surface-modified nanofibrous biomaterial bridge for the enhancement and control of neurite outgrowth. Biointerphases 2010;5(4):149–58. https://doi.org/10.1116/1.3526140.
[29] Raheleh S, Masoud S, Adeleh D, Akram E, Abdolreza A. Biological behavior study of gelatin coated PCL nanofiberous electrospun scaffolds using fibroblasts. Journal of Paramedic Sci 2014:67–73.
[30] Tan E, Ng S, Lim C. Tensile testing of a single ultrafine polymeric fiber. Biomaterials 2005;26:1453–6. https://doi.org/10.1016/j.biomaterials.2004.05.021.
[31] Barrera S. Obtención de nanofibras modificadas de poli(e-caprolactona) por electrohilado para aplicaciones biomédicas. Instituto de Investigaciones en Materiales. Universidad Nacional Autónoma de México; 2014.
[32] Maleki M, Natalello A, Pugliese R, Gelain F. Fabrication of nanofibrous electrospun scaffolds from a heterogeneous library of co-and self-assembling peptides. Acta Biomater 2017;51:268–78. https://doi.org/10.1016/j.actbio.2017.01.038.
[33] Ulery BD, Nair LS, Laurencin CT. Biomedical appli- cations of biodegradable polymers. J Polym Sci B Polym Phys 2011;49:832–64. https://doi.org/10.1002/polb.22259.
[34] Elzoghby A. Gelatin-based nanoparticles as drug and gene delivery systems: reviewing three decades of research. J Control Rel 2013;172(3):1075–91. https://doi.org/10.1016/j.jconrel.2013.09.019.
[35] Ardeshirylajimi A, Hosseinkhani S, Parivar K, Yaghmaie P, Soleimani M. Nanofiber-based polyethersulfone scaffold and efficient differentiation of human induced pluripotent stem cells into osteoblastic lineage. Mol. Biol. Rep. 2013:1–8. https://doi.org/10.1007/s11033-013-2515-5.
[36] Ravichandran R, Venugopal JR, Sundarrajan S, Mukherjee S, Ramakrishna S. Poly (glycerol sebacate)/gelatin core/shell fibrous structure for regeneration of myocardial infarction. Tissue Eng Part A 2011;17(9−10):1363–73. https://doi.org/10.1089/ten.TEA.2010.0441.
[37] Shin H, Lee C, Cho I, Kim Y, Lee Y, Kim I, et al. Electrospun PLGA nanofiber scaffolds for articular cartilage reconstruction: mechanical stability, degradation and cellular responses under mechanical stimulation in vitro. J Biomater Sci Polym Edit. 2006;17(1−2):103–19. https://doi.org/10.1163/156856206774879126.
[38] Beachley V, Wen X. Polymer nanofibrous structures: fabrication, biofunctionalization, and cell interactions. Prog Polym Sci 2010;35(7):868–92. https://doi.org/10.1016/j.progpolymsci.2010.03.003.
[39] Vasita R, Katti DS. Nanofibers and their applications in tissue engineering. Int J Nanomed 2006;1(1):15–30. https://doi.org/10.2147/nano.2006.1.1.15.